ECCOMAS Congress 2016
VII European Congress on Computational Methods in Applied Sciences and Engineering
M. Papadrakakis, V. Papadopoulos, G. Stefanou, V. Plevris (eds.)
Crete Island, Greece, 5–10 June 2016

ADJOINT OPTIMAL CONTROL PROBLEMS FOR FLUID-STRUCTURE INTERACTION SYSTEMS

D. Cerroni[1], R. Da Vià[1], S. Manservisi[1], F. Menghini[1*], and L. Zaniboni

[1]University of Bologna
Via dei Colli 16, Laboratory of Montecuccolino - DIN

[*] e-mail: filippo.menghini3@unibo.it

Keywords: Adjoint Optimal Control, Fluid-Structure Interaction.

Abstract. *In the last years adjoint optimal control has been increasingly used for design and simulations in several research fields. Applications to Computational Fluid Dynamics problems dedicated to the study of transient-diffusion equations, shape optimization problems, fluid-solid conjugate heat transfer and turbulent flows can be found in literature. The study of Fluid-Structure Interaction problems gained popularity recently because of many interesting applications in engineering and biomedical fields. In this paper we study adjoint optimal control problems for Fluid-Structure Interaction systems in order to improve the advantages of using FSI simulations when designing engineering devices where fluid-dynamical interactions between a fluid and a solid play a significant role. We assess distributed optimal control problems with the purpose to control the fluid behavior by moving the solid region to obtain a desired fluid velocity in specific parts of the domain. The adjoint equations of the FSI monolithic system are derived and the optimality system solved for some simple cases with an in-house finite element code with mesh-moving capabilities for the study of large displacements in the solid. The approach presented in this work is general and can be used to assess different objectives and types of control in future works.*

1 INTRODUCTION

Optimization has always been used to improve the performance of engineering devices. Nowadays several approaches to optimization are available, such as single and multi-objective, adjoint or sensitivities based method, evolutionary algorithms and many others. In literature there are several works dealing with this subject, for a quick review the interested reader can see [1, 2, 3, 4, 5, 6, 7, 8] and references therein.

Fluid-Structure Interaction (FSI) problems can be defined as a system where the fluid flow alters the tensional state of a solid moving shape and the solid deformation has an important effect on the fluid flow. Examples of this type of systems are quite common in engineering, like floating structures, wind turbines, man-made drones and in the study of biological systems such as artery or heart valves. In literature these topics are investigated deeply and the interested reader can see [9, 10, 11, 12, 13, 14]. Many attempts to use optimization techniques can be found, for example in [15], where the authors propose a solution method for the problem of optimizing a non-linear aeroelasticity system in a steady-state flow by using a sensitivity method. The work in [16] deals with general shape optimization methods based on design sensitivity analysis. In [17] a partitioned approach for a NURBS-parametrized shape optimization problem is studied. In the recent work [18] the authors propose a reduced order model, based on a sequential quadratic programming approach, to accelerate the shape optimization process.

In this work we focus on adjoint based optimal control approach which is very popular in industrial applications where Computational Fluid Dynamics simulations should be performed [19, 20, 21, 22, 23]. Moreover this method has a solid mathematical background and the existence of local optimal solutions can be investigated in many interesting cases, see for examples [21, 22, 24]. We are interested in a monolithic approach to the solution of the FSI system leading to a stable and well defined solution in a finite element setting [25, 26]. Inside this framework we study a distributed optimal control problem applied to the monolithic FSI system. The objective of the control is a velocity profile matching in a specific region of the domain. This is accomplished by enforcing a force in the solid domain which deforms the shape and thus the fluid flow profile. In the next section we derive the optimality system which consists of the state, the adjoint system and the control equation. In order to solve the optimality system we propose a simple steepest descent algorithm. In Section 3 we report some numerical results obtained by the implementation of the optimal control algorithm in a finite element parallel code designed for multiphysics simulations.

2 OPTIMALITY SYSTEM

In this section we present the mathematical model of the FSI problem together with the derivation of the optimality system. We use standard notation $H^s(\Omega)$ for the Sobolev spaces with norm $\|\cdot\|_s$ ($H^0(\Omega) = L^2(\Omega)$ and $\|\cdot\|_0 = \|\cdot\|$). Let $H^s_0(\Omega)$ be the space of all functions in $H^s(\Omega)$ that vanish on the boundary Γ_d of the bounded open set Ω and $H^{-s}(\Omega)$ be the dual space of $H^s_0(\Omega)$. The trace space for the functions in $H^1(\Omega)$ is denoted by $H^{1/2}(\Gamma)$.

Let us consider the domain $\Omega \subset R^N$ which consists of a fluid Ω^f and a solid part Ω^s. The solid domain is defined through the solid displacement field $\mathbf{l}$ as

$$\Omega^s(\mathbf{l}) = \{\mathbf{x} \in R^3 \text{ such that } \mathbf{x} = \mathbf{x}_0 + \mathbf{l}\}\,. \tag{1}$$

The position vector $\mathbf{x}_0$ defines the initial solid domain Ω^s_0 before the deformation $\mathbf{l}$. We write $\Omega^s(\mathbf{l})$ for the final domain and $\Omega^s(\mathbf{0}) = \Omega^s_0$ for the initial undeformed domain. In the rest of the paper we drop the notation $(\mathbf{l})$ and $(\mathbf{0})$ over the domain whenever it is not necessary.

The mathematical model of the steady state FSI problem in strong form is

$$\boldsymbol{\nabla} \cdot \mathbf{v} = 0 \qquad \text{on} \quad \Omega^f \,, \tag{2}$$

$$\rho(\mathbf{v} \cdot \boldsymbol{\nabla})\mathbf{v} - \boldsymbol{\nabla} \cdot \mathbf{T} - \mathbf{f}_f = 0 \qquad \text{on} \quad \Omega^f \,, \tag{3}$$

$$\boldsymbol{\nabla} \cdot \mathbf{S}(\mathbf{l}) + \mathbf{f}_s = 0 \qquad \text{on} \quad \Omega^s \,, \tag{4}$$

where $\mathbf{v}$ is the fluid velocity, ρ the fluid density, $\mathbf{T}$ the viscous stress tensor of the fluid, $\mathbf{S}$ the strain tensor of the solid, $\mathbf{f}$ a force acting on the solid and Ω^f and Ω^s the fluid and solid domain, respectively. The tensors $\mathbf{T}$ and $\mathbf{S}$ have to be defined by a constitutive model. A simple choice is a Newtonian fluid for $\mathbf{T}$ and a linear elastic solid for $\mathbf{S}$,

$$\mathbf{T}(p, \mathbf{v}) = -p\mathbf{I} + \mu_l \boldsymbol{\nabla}\mathbf{v} \,, \tag{5}$$

$$\mathbf{S}(\mathbf{l}) = \lambda_s(\boldsymbol{\nabla} \cdot \mathbf{l})\mathbf{I} + \mu_s \boldsymbol{\nabla}\mathbf{l} \,, \tag{6}$$

where p is the fluid pressure, μ_l is the dynamic viscosity of the fluid and λ_s and μ_s are the first and second Lamè parameters of the solid. When the parameter $\lambda \to \infty$ the solid becomes incompressible and another equation is needed for the incompressibility constraint. In the following we study incompressible solid materials only.

The system (2-4) has to be completed with appropriate boundary and interface conditions, which are

$$\begin{aligned}
\mathbf{v} &= \mathbf{v_0} && \text{on} && \Gamma_{fd} \,, \\
\mathbf{l} &= \mathbf{l_0} && \text{on} && \Gamma_{sd} \,, \\
\mathbf{T} \cdot \mathbf{n} &= \mathbf{0} && \text{on} && \Gamma_{fn} \,, \\
\mathbf{S} \cdot \mathbf{n} &= \mathbf{0} && \text{on} && \Gamma_{sn} \,, \\
\mathbf{T} \cdot \mathbf{n} &= \mathbf{S} \cdot \mathbf{n} && \text{on} && \Gamma_{i} \,, \\
\mathbf{v} &= \mathbf{0} && \text{on} && \Gamma_{i} \,,
\end{aligned} \tag{7}$$

where Γ_{fd} and Γ_{sd} are the surfaces where a Dirichlet boundary condition is imposed for the fluid velocity and solid displacement, Γ_{fn} and Γ_{sn} are the surfaces where Neumann homogenous conditions are imposed for both the fields and Γ_i is the interface between the solid and the fluid domain, $\Gamma_i = \Omega^f \cap \Omega^s$. In FSI problems the boundary conditions are of primary importance because conditions on the fluid-solid interface can lead to convergence issues so they must be correctly imposed. It is very common to solve FSI problems using dedicated solvers for the fluid and solid domains. This method is called segregated approach and it is widely used in commercial CFD codes. A known drawback of this method is the need to impose interface conditions in an iterative way because the two solvers are coupled through the field values on the interface which give the appropriate boundary conditions to the other solver. This approach can lead to convergence issues, especially when large deformations occur in the solution. On the other hand, by using a monolithic approach with a finite element method, the interface conditions are imposed directly in the same solver and there is no need to iterate to obtain the correct interface values. In this work we use a monolithic approach, so the same solver is used for both the fluid and the solid domain. However the derivation of the optimality system is performed *a priori* and though is valid for both segregated and monolithic approaches.

To derive the optimality system with the Lagrange multiplier method we first establish the objective of the control. In this work we study a fluid velocity matching problem in which the control is a force inside the solid domain. This can be done since we have a complete FSI

formulation in which the fluid and solid domains are considered in the mathematical model definition. The objective or cost functional can be defined

$$\mathcal{J}(\mathbf{v},\mathbf{f}) = \frac{1}{2}\int_{\Omega^d} w\,(\mathbf{v}-\mathbf{v}_d)^2\,d\Omega + \frac{1}{2}\int_{\Omega^c} \beta\,\mathbf{f}^2\,d\Omega\,. \tag{8}$$

The function w is a weight function of the coordinate $\mathbf{x}$ which can be used to set a control in a specific region of the fluid domain. The positive number β is a regularization parameter which is needed in the optimal control formulation to obtain a control function in the space of non singular integrable functions $L^2(\Omega^c)$. If a too high value of β is chosen the control becomes too smooth and the objective cannot be achieved well, while convergence problems can arise in the numerical solution of the problem if β is chosen too low.

In order to derive the optimality system we write the full constrained Lagrangian of the problem which consists of the objective functional and state equations multiplied by the appropriate Lagrangian multipliers

$$\begin{aligned}\mathcal{L}(p,\mathbf{v},\mathbf{l},\widehat{\mathbf{l}},\mathbf{f},p_a,\mathbf{v}_a,\widehat{\mathbf{l}}_a,\widehat{\mathbf{s}}_a,\boldsymbol{\beta}_a) = \mathcal{J}(\mathbf{v},\mathbf{f}) + \int_{\Omega^f}(\nabla\cdot\mathbf{v})\,p_a\,d\Omega + \\ \int_{\Omega^f}[(\rho(\mathbf{v}\cdot\nabla)\mathbf{v}) + \boldsymbol{\nabla} p + \boldsymbol{\nabla}\cdot(\mu_f\boldsymbol{\nabla}\mathbf{v})]\cdot\boldsymbol{v}_a\,d\Omega + \\ \int_{\Omega^s}[-\boldsymbol{\nabla}\cdot(\mu_s\boldsymbol{\nabla}\mathbf{l}+\lambda_s\mathbf{I}(\nabla\cdot\mathbf{l})) - \mathbf{f}]\cdot\boldsymbol{v}_a\,d\Omega + \int_{\Omega^s}\boldsymbol{\nabla}^2\widehat{\mathbf{l}}\cdot\widehat{\mathbf{l}}_a\,d\Omega + \\ \int_{\Gamma_i}\widehat{\mathbf{s}}_a\cdot\left[(\widehat{\mathbf{l}}-\mathbf{l}) + \frac{\mathbf{v}}{h}\right]d\Gamma + \int_{\Omega^s}\boldsymbol{\beta}_a\cdot\left[\mathbf{v}-h(\mathbf{l}-\widehat{\mathbf{l}})\right]d\Omega\,.\end{aligned} \tag{9}$$

In (9) the auxiliary mesh displacement field $\widehat{\mathbf{l}}$ is defined over the solid domain $\Omega^s(\mathbf{l})$, which is the solution of a Laplacian operator. Moreover the velocity field is defined also on the solid domain through the last term in (9). By taking the Frèchet derivatives of (9) with respect to the adjoint variables we recover the state system (2-4) in weak form with the correct boundary and interface conditions. When the derivatives are taken with respect to the state variables and some simplifications are performed on the equations, the adjoint system in weak form reads

$$\int_{\Omega^f}\delta p\boldsymbol{\nabla}\cdot\mathbf{v}_a\,d\Omega = 0 \qquad \forall\delta p\in L^2(\Omega^f)\,, \tag{10}$$

$$\begin{aligned}\int_{\Omega^d}(\mathbf{v}-\mathbf{v}_d)\cdot\delta\mathbf{v}\,d\Omega + \int_{\Omega^s}[\mu_s\boldsymbol{\nabla}\boldsymbol{v}_a:\boldsymbol{\nabla}\delta\mathbf{v} + \lambda_s(\boldsymbol{\nabla}\cdot\boldsymbol{v}_a)(\boldsymbol{\nabla}\cdot\delta\mathbf{v})]\,d\Omega + \\ \int_{\Omega^f}(\boldsymbol{\nabla}\cdot\delta\mathbf{v})\,p_a\,d\Omega + \int_{\Omega^f}[(\rho(\delta\mathbf{v}\cdot\boldsymbol{\nabla})\mathbf{v})\cdot\boldsymbol{v}_a + (\rho(\mathbf{v}\cdot\boldsymbol{\nabla})\delta\mathbf{v})\cdot\boldsymbol{v}_a + \\ \mu_f\boldsymbol{\nabla}\boldsymbol{v}_a:\boldsymbol{\nabla}\delta\mathbf{v}]\,d\Omega = 0 \qquad \forall\delta\mathbf{v}\in\mathbf{H}^1_{\Gamma_d^f\cup\Gamma_d^s}(\Omega)\,,\end{aligned} \tag{11}$$

The shape derivatives with respect to the fluid and solid domain are taken into account. Since Ω^d and Ω^c are fixed and the system is solved by using a monolithic approach then the shape derivative contribution can be only seen in the $\mathbf{l}_a$ adjoint equation. We do not need the solution of the $\mathbf{l}_a$ adjoint equation to compute the distributed control $\mathbf{f}$ and therefore it is not reported. We remark that the use of a segregated approach, where the solid and the fluid are solved on separated domains, needs to take into account of shape derivatives which appear split into two contributions on different domains. This is one of the main advantage of the monolithic approach.

If one is interested in the strong form of the *adjoint system*, for instance to obtain a proper finite volume discretization, it is necessary to perform some integrations by parts on the terms where the variations δ are differentiated. After performing the integration by parts, we recover the adjoint state $(\mathbf{v}_a^f, \mathbf{v}_a^s, p_a) \in \mathbf{H}^1_{\partial\Omega^f - \Gamma_i}(\Omega^f) \cap \mathbf{H}^2(\Omega^f) \times \mathbf{H}^1_{\partial\Omega^s - \Gamma_i}(\Omega^s) \cap \mathbf{H}^2(\Omega^s) \times L^2_0(\Omega^f) \cap \mathbf{H}^1(\Omega^f)$, by solving

$$\boldsymbol{\nabla} \cdot \mathbf{v}_a^f = 0\,, \tag{12}$$

$$-\rho(\boldsymbol{\nabla}\mathbf{v})^T\mathbf{v}_a^f + \rho[(\mathbf{v}\cdot\boldsymbol{\nabla})\mathbf{v}_a^f] + \boldsymbol{\nabla} p_a - \boldsymbol{\nabla}\cdot(\mu_l \boldsymbol{\nabla}\mathbf{v}_a^f) = w(\mathbf{v}-\mathbf{v}_d)\,, \tag{13}$$

$$\boldsymbol{\nabla}\cdot\mathbf{S}(\mathbf{v}_a^s) = 0\,. \tag{14}$$

with boundary conditions defined as

$$\mathbf{v}_a^s = \mathbf{v}_a^f \qquad \text{on } \Gamma_i \tag{15}$$

$$\mathbf{S}(\mathbf{v}_a^s)\cdot\mathbf{n} = \left(\mu_l(\boldsymbol{\nabla}\mathbf{v}_a^f + (\boldsymbol{\nabla}\mathbf{v}_a^f)^T) - p_a\right)\cdot\mathbf{n} \qquad \text{on } \Gamma_i \tag{16}$$

$$\mu_l(\boldsymbol{\nabla}\mathbf{v}_a)\cdot\mathbf{n} = -(\mathbf{v}\cdot\mathbf{n})\,\mathbf{v}_a\,, \qquad p_a = 0 \qquad \text{on } \Gamma_{fn}\,. \tag{17}$$

To obtain the definition of the control $\mathbf{f}$ we take the derivative of 9 with respect to $\mathbf{f}$ and we have

$$\mathbf{f} = \mathbf{v}_a/\beta\,. \tag{18}$$

The distributed control is then equal to the adjoint variable $\mathbf{v}_a$ scaled by the regularization parameter β.

We use the following steepest descent algorithm to solve the optimal control problem. In Algorithm 1 we set the tolerance on the optimal control convergence $\tau = 10^{-6}$. The step length r allows us to under-relax the solution of the optimal control problem and to avoid

Algorithm 1 Steepest descent algorithm to find the optimal solution

function FIND OPTIMAL
  set a state $(\mathbf{v}^0, p^0, \mathbf{l}^0)$ satisfying (2-4) ▷ *Setup of the state - Reference case*
  compute the functional $\mathcal{J}^0$ in (8)
  set $\mathbf{f}^0 = 0, r^0 = r_0$
  for $i = 1 \to i_{max}$ **do**
    Solve the system (10)-(11) to obtain the adjoint state $(\mathbf{v}_a^i, p_a^i)$
    for $j = 1 \to j_{max}$ **do**
      compute the control $\mathbf{f}^i = \mathbf{f}^{i-1} + r^{i,j}\,\mathbf{v}_a^i/\beta$
      solve (2-4) for the state $(\mathbf{v}^{i,j}, p^{i,j}, \mathbf{l}^{i,j})$ with the new control $\mathbf{f}^i$.
      compute the new functional $\mathcal{J}^{i,j+1}$ in (8)
      if $\|\mathcal{J}^{i,j+1} - \mathcal{J}^{i,j}\|/\mathcal{J}^{i,j} < \tau$ **then**
        convergence reached ▷ *end of the algorithm*
      else if $\mathcal{J}^{i,j+1} > \mathcal{J}^{i,j}$ **then**
        set $r^{i,j+1} = 2/3\, r^{i,j}$, $j = j+1$ and go to 8 ▷ *loop on j again*
      else if $\mathcal{J}^{i,j+1} < \mathcal{J}^{i,j}$ **then**
        set $r^{i,j+1} = 3/2\, r^{i,j}$, $i = i+1$ and go to 6 ▷ *loop on i again*
      end if
    end for
  end for
end function

strong oscillations. In the loop j, the search of a decreasing functional, we solve iteratively the state system by adjusting this parameter in order to obtain a proper decrease of the functional. When this is accomplished we save the control and we iterate again on the main loop i where the adjoint system is solved. This algorithm requires several solutions of the state and adjoint systems in order to find the optimal control, however it does not need a great amount of memory which is limited to a standard CFD simulation.

We implemented this algorithm in a finite element code which is parallelized with openMPI libraries and uses a multigrid solver with mesh-moving capability [26, 27]. We have used standard Taylor-Hood finite elements for the velocity and pressure solution in order to fulfill the inf-sup condition and a SUPG stabilization technique. The displacements are approximated with standard quadratic elements. In the following we report the results obtained with the proposed algorithm in some simple test cases. First we overview the reference FSI problem with no control, then report the optimal solutions found for different objective velocity profiles and values of β ranging from 10^{-2} to 10^{-6}. The test case setting and the results are presented in a non-dimensional form.

3 NUMERICAL RESULTS

In this section we report the numerical results obtained by applying Algorithm 1 to a two-dimensional test case. The geometry of the test case is shown in Figure 1, where the blue region represents the fluid and the red region of the solid domain. The inlet of the flow is defined by the green line AB, the outlets by the two black lines CD and EF on the right. The overall domain is

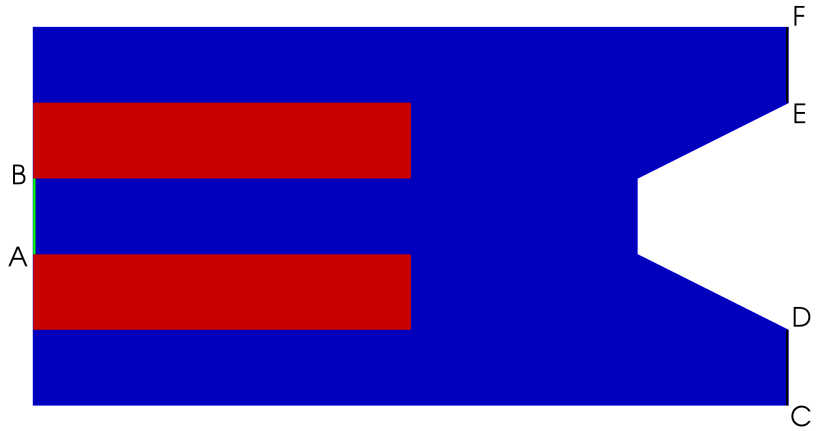

Figure 1: Geometry of the test case. The blue region is the fluid and the red one is the solid domain. On the left the green line AB is the inlet, on the right the black lines CD and EF are the outlets of the flow. The rest of the boundary is a non deformable solid wall.

Property	value	Property	value
E	2×10^2	μ	1×10^{-2}
ρ_s	1	ρ_l	1

Table 1: Physical data for the solid and the fluid.

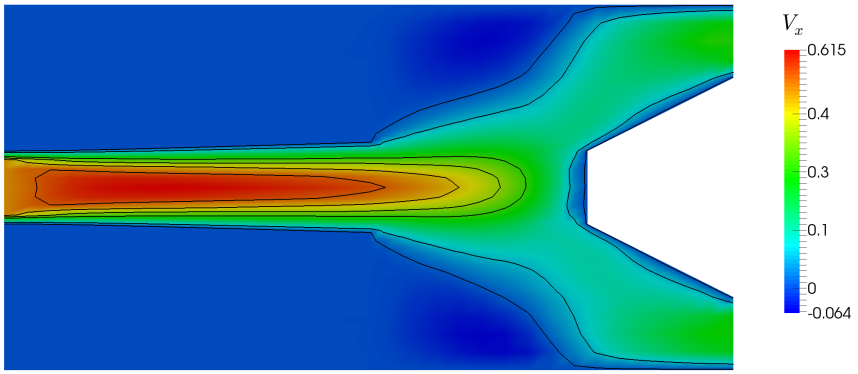

Figure 2: Axial velocity of the reference test case. The velocity v_x is reported with colors and with six lines of iso-magnitude.

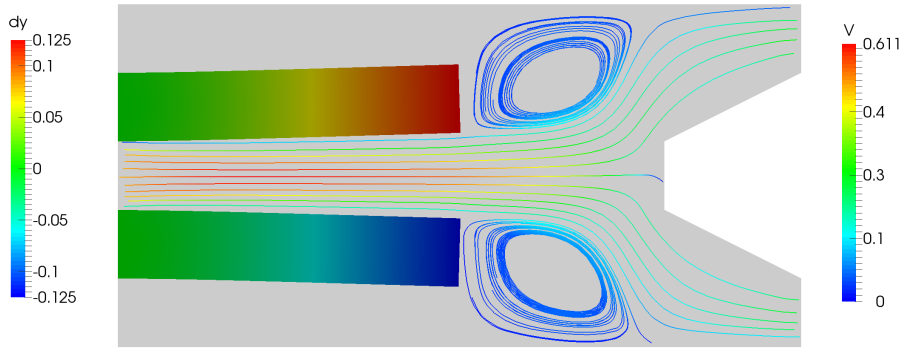

Figure 3: Reference test case, flow field and displacement in the vertical direction. The streamlines are colored with the velocity magnitude and the displacement in the vertical direction dy is reported on the solid bar with colors.

10 wide on the x-axis and 5 high on the y-axis, while lines AB, CD and EF are 1 long each.

The fluid enters from the left with a flat profile, it develops in the region between the two solid bars and hits the solid non deformable wall on the right where the flow is split in two equal secondary flows that leave the domain from the bottom and the outlets on the right. The inlet velocity is set to $\mathbf{v} = (0.5, 0)$ and the other boundaries are considered non deformable solid walls, so the velocity is $\mathbf{v} = (0, 0)$. The solid bars have a boundary that is assumed to be non deformable, so here the solid displacement is set to $\mathbf{l} = (0, 0)$. The physical properties are reported in Table 1. Given these properties, the inlet velocity and the transverse length we can compute the Reynolds number of the flow as $Re = 500$.

We first report the reference flow field without control and then set up the optimal control problem. In Figure 2 the axial velocity v_x is reported with colors and with six lines of iso-magnitude. The flow is accelerated between the two solid bars and then it slows down and split

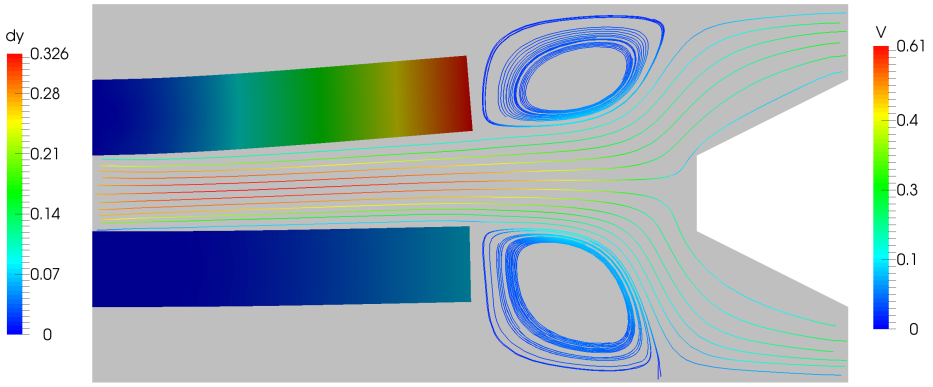

Figure 4: Controlled test case with $\mathbf{v}_{d1}$ and $\beta = 10^{-6}$, flow field and displacement in the vertical direction. The streamlines are colored with the velocity magnitude and the displacement in the vertical direction dy is reported on the solid bar with colors.

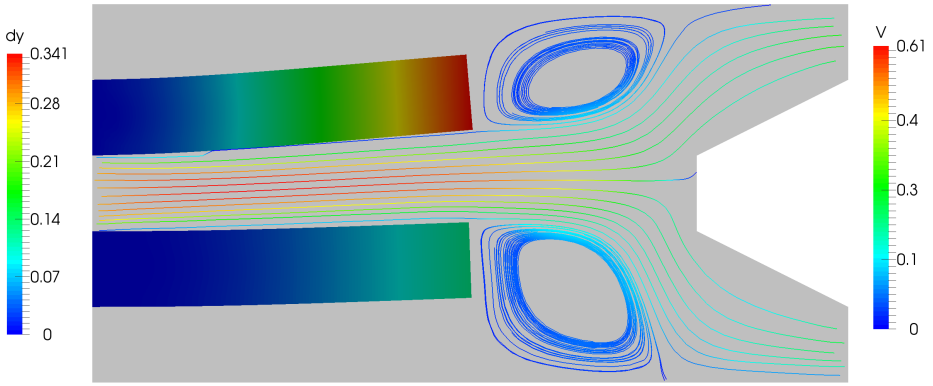

Figure 5: Controlled test case with $\mathbf{v}_{d2}$ and $\beta = 10^{-6}$, flow field and displacement in the vertical direction. The streamlines are colored with the velocity magnitude and the displacement in the vertical direction dy is reported on the solid bar with colors.

before leaving the domain with an average velocity around 0.2. In Figure 3 the streamlines of the velocity field are reported and colored with the magnitude of the velocity field. With this visualization of the flow two slow recirculation vortexes appear in the region near the tips of the solid bars. The solid bars displacement can be seen in this Figure and the value of $\mathbf{l}_y = dy$ is reported with colors on the solid bars. The whole problem is symmetrical with respect to the line $y = 2.5$.

To obtain a proper benchmark for our Algorithm we assign the objective of the functional

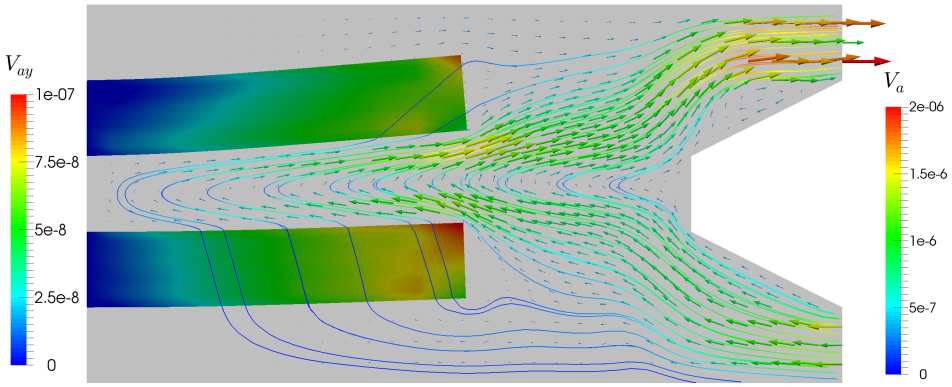

Figure 6: Controlled test case with $\mathbf{v}_{d2}$ and $\beta = 10^{-6}$, adjoint velocity field. The streamlines and arrows are colored with the adjoint velocity magnitude and in the solid bars the vertical adjoint variable is reported with a different color scale.

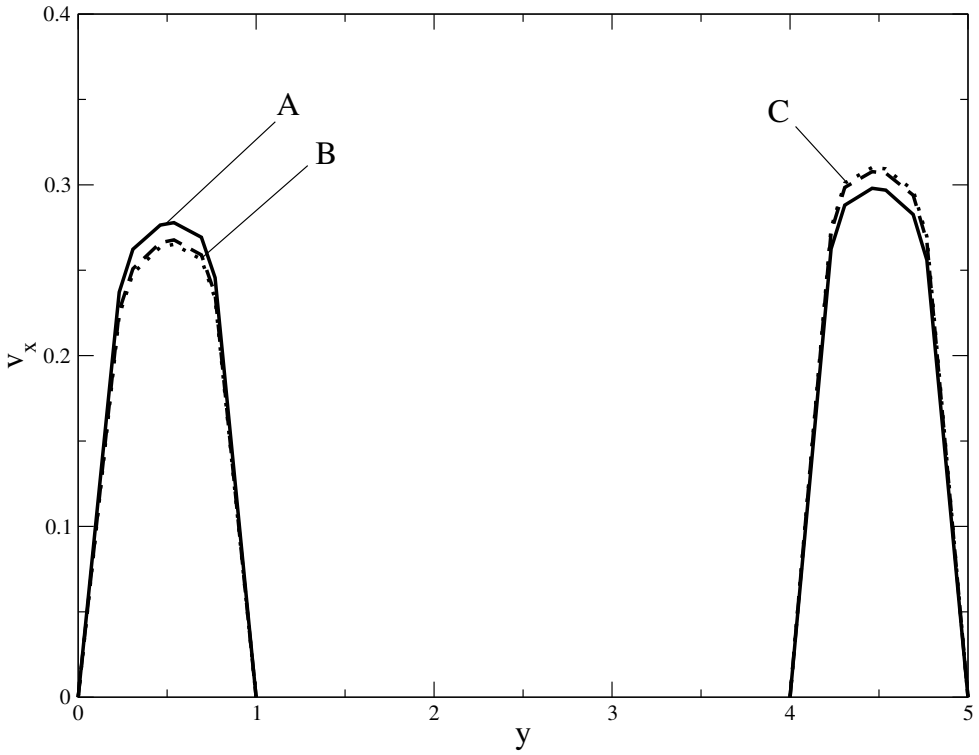

Figure 7: Axial velocity v_x plotted on a vertical line at $x = 10$, comparison between reference case (A, continuous line), test case with $\mathbf{v}_{d1}$ and $\beta = 10^{-6}$ (B, dashed line) and test case with $\mathbf{v}_{d2}$ and $\beta = 10^{-6}$ (C, dotted line).

with a weight function

$$w(\mathbf{x}) = \begin{cases} 1 & \text{if} \quad x > 9, y > 4 \\ 0 & \text{otherwise} \end{cases} \tag{19}$$

and set the desired velocity $\mathbf{v}_{d1} = (0.25, 0)$ or $\mathbf{v}_{d2} = (0.4, 0)$ in this region. By doing so we aim at breaking the symmetry of the problem by increasing the axial velocity near the upper outlet.

β	∞	10^{-2}	10^{-4}	10^{-6}
Case with $\mathbf{v}_{d1}$	0.00521914	0.00519039	0.00511677	0.00511527
Case with $\mathbf{v}_{d2}$	0.0312969	0.0297863	0.0295657	0.0295634

Table 2: Objective functionals computed with different β values in the test cases with $\mathbf{v}_{d1}$ and $\mathbf{v}_{d2}$. The reference case with no control is labeled with $\beta = \infty$.

The optimal control problem has been studied for the two desired velocities $\mathbf{v}_{d1}$ and $\mathbf{v}_{d2}$ and for three values of the parameter $\beta = 10^{-2}$, 10^{-4} and 10^{-6}. In Figure 4 the results of the algorithm obtained by using $\mathbf{v}_{d1}$ and $\beta = 10^{-6}$ are reported with streamlines that visualizes the flow field and with the displacement in the vertical direction $\mathbf{l}_y = dy$. The controlling force pushes the bars upper and changes their shape allowing the fluid to be mainly directed towards the upper outlet thus increasing the axial velocity in this region. Also the vortexes change, with the one on the bottom becoming wider than the upper one. In order to improve the control power we can use $\mathbf{v}_{d2}$. In Figure 5 we report the results of the optimal control algorithm by using $\mathbf{v}_{d2}$ and $\beta = 10^{-6}$. The main flow is very similar to the one depicted in Figure 4, the differences lying in a higher displacement in the vertical direction $\mathbf{l}_y = dy$ with the bottom bar displaced too and in a more pronounced flow pattern towards the upper outlet. The adjoint velocity is the controlling force in the solid domain but its source is located in the fluid domain. In Figure 6 this variable is reported with streamlines and arrows colored with its magnitude to visualize the adjoint flow field in the test case with $\mathbf{v}_{d2}$ and $\beta = 10^{-6}$. In the solid bars the vertical adjoint velocity is reported with colors and rescaled. The adjoint flow field enters the domain from the bottom outlet, it develops inside the two bars, crosses them in the internal region and then exits through the upper outlet. One has to keep in mind that the value of the adjoint velocity is related with the value of β since the physical controlling force that is used in the state FSI problem is the adjoint divided by β.

We report in Figure 7 a plot of the axial velocity v_x on a vertical line parallel to the y-axis at $x = 10$, on the outlet. The reference result is reported with a continuous line and it is compared with the controlled result obtained by using $\mathbf{v}_{d1}$ (dashed line) and $\mathbf{v}_{d2}$ (dotted line), both with $\beta = 10^{-6}$. A small asymmetry can be seen in the reference case between the upper and the bottom velocities. However this is negligible compared with the clear velocity increasing that can be seen in the upper outlet in the controlled cases and this is followed by a flow decreasing on the bottom outlet, due to the mass conservation constraint. To gain a more quantitative comparison of the results we report in Table 2 the objective functional (8) as computed in the reference and in the controlled cases, with the different β. One can appreciate the decrease in the functional in both the test cases with decreasing β. We can therefore conclude that the optimal control algorithm is performing well in the search of a minimum of the objective functional. However the movement of the solid cannot increase or decrease in large amount the outlet velocity due to the mass constraint at the inlet.

4 CONCLUSION

In this work a distributed optimal control for the fluid-structure interaction problem has been studied. The objective of the optimal control problem is a velocity matching profile in a specific region of the fluid domain and the control acts through a force in the solid that changes the shape of the solid domain. The optimality system has been derived from the complete Lagrangian of the problem and an algorithm for the numerical solution of this system has been presented. The results obtained show the feasibility of this approach and the possible use of this method in

many industrially relevant applications. However some improvements are needed in the FSI solver because too large deformations with small change in topology are not allowed unless remeshing or more complex techniques are used to handle this problem. With this limitation the optimal control algorithm might not find the local minimum if this is obtained with a large shape change. Nevertheless this algorithm is useful to obtain a reduction in the objective functional that can be a first step in industrial design and the shape cannot be changed dramatically due to other constraints. In future works we plan to assess other objectives and types of control in order to better show the capability of this optimization approach for the design and improvement of engineering devices where the interaction between fluid and solid plays a significant role.

REFERENCES

[1] A. Chinchuluun, P.M. Pardalos, R. Enkhbat, I. Tseveendorj, *Optimization and Optimal Control: Theory and Applications*, Springer Optimization and Its Applications, Springer, 2010.

[2] B.R. Noack, M. Morzynski, G. Tadmor, *Reduced-Order Modelling for Flow Control*, CISM International Centre for Mechanical Sciences, Springer, 2011.

[3] G. Leugering, S. Engell, A. Griewank, M. Hinze, R. Rannacher, V. Schulz, M. Ulbrich, S. Ulbrich, *Constrained Optimization and Optimal Control for Partial Differential Equations*, International Series of Numerical Mathematics, Birkhäuser Mathematics, Springer, 2012.

[4] J. Nocedal and S. J. Wright, *Numerical Optimization*, Springer Series in Operation Research and Financial Engineering, Springer, 2006.

[5] M.D. Gunzburger, *Perspectives in Flow Control and Optimization*, Advances in Design and Control, SIAM, 2003.

[6] C.W. Rowley and D.R. Williams, *Dynamics and Control of High-Reynolds-Number Flow over Open Cavities*, Annual Review of Fluid Mechanics, vol. 38, pp. 251-276, 2006.

[7] J. Kim and T.R. Bewley, *A Linear Systems Approach to Flow Control*, Annual Review of Fluid Mechanics, vol. 39, pp. 383-417, 2007.

[8] M Gunzburger and S Manservisi, *Analysis and approximation for linear feedback control for tracking the velocity in Navier-Stokes flows*, Computer Methods in Applied Mechanics and Engineering, Volume 189 (3), pp. 803-823 (2000)

[9] S. Turek, J. Hron, *Proposal for Numerical Benchmarking of Fluid-Structure Interaction between an Elastic Object and Laminar Incompressible Flow*, Lecture Notes in Computational Science and Engineering, Vol. 53, pp. 371-385, 2006.

[10] L. Formaggia, A. Quarteroni and A. Veneziani, *Cardiovascular Mathematics*, Springer, 2009.

[11] P. Tallec and J. Mouro, *Fluid structure interaction with large structural displacements*, Computer Methods in Applied Mechanics and Engineering, Vol. 190 (24-25), pp. 3039-3067, 2001.

[12] M. Bukaè, S. Čaniè and B. Muha, *A partitioned scheme for fluid-composite structure interaction problems*, Journal of Computational Physics, Vol. 281, pp. 493-517, 2015.

[13] A. Gilmanova, T.B. Lea, F. Sotiropoulos, *A numerical approach for simulating fluid structure interaction of flexible thin shells undergoing arbitrarily large deformations in complex domains*, Journal of Computational Physics, Vol. 300, pp. 814-843, 2015.

[14] A. Calderer, S. Kang, F. Sotiropoulos, *Level set immersed boundary method for coupled simulation of air/water interaction with complex floating structures*, Journal of Computational Physics, Vol. 277, pp. 201-227, 2014.

[15] K. Maute, M. Nikbay and C. Farhat, *Sensitivity analysis and design optimization of three-dimensional nonlinear aeroelastic systems by the adjoint method*, International Journal for Numerical Methods in Engineering, Vol. 56 (6), pp. 911-933, 2003.

[16] E. Lund, H. Moller and L.A. Jakobsen, *Shape design optimization of stationary fluid-structure interaction problems with large displacements and turbulence*, Structural and Multidisciplinary Optimization, Vol. 25 (5), pp. 383-392, 2003.

[17] M. Hojjat, E. Stavropoulou, T. Gallinger, U. Israel, R. Wüchner, K.U. Bletzinger, *Fluid-structure interaction in the context of shape optimization and computational wind engineering*, Fluid Structure Interaction II, Vol. 73, pp. 351-381, 2010.

[18] N. Aghajari and M. Schäfer, *Efficient shape optimization for fluid-structure interaction problems*, Journal of Fluids and Structures, Vol. 57, pp. 298-313, 2015.

[19] Y. Yan and D.E. Keyes, *Smooth and robust solutions for Dirichlet boundary control of fluid-solid conjugate heat transfer problems*, Journal of Computational Physics, vol. 281, pp. 759-786, 2015.

[20] E.M. Papoutsis-Kiachagiasa, S.A. Kyriacoua, and K.C. Giannakogloua, *The continuous adjoint method for the design of hydraulic turbomachines*, Computer Methods in Applied Mechanics and Engineering, Vol. 278, pp. 621-639, 2014.

[21] M. Gunzburger and S. Manservisi, *Analysis and approximation of the velocity tracking problem for Navier-Stokes flows with distributed control*, SIAM Journal of Numerical Analysis, vol. 37 (5), pp. 1481-1512, 2000.

[22] M. Gunzburger and S. Manservisi, *The velocity tracking problem for Navier-Stokes flow with boundary control*, SIAM Journal on Control and Optimization, vol. 39 (2), pp. 594-634, 2000.

[23] S. Manservisi and F. Menghini, *Numerical simulations of optimal control problems for the Reynolds averaged Navier-Stokes system closed with a two-equation turbulence model*, Computers & Fluids, Vol. 125, pp. 130-143, 2016.

[24] S. Manservisi and F. Menghini, *Optimal control problems for the Navier-Stokes system coupled with the k-ω turbulence model*, Computers & Mathematics with Applications, 2015 doi:10.1016/j.camwa.2015.10.003

[25] J. Hron and S. Turek, *A monolithic FEM/multigrid solver for an ALE formulation of fluid-structure interaction with applications in biomechanics* Fluid-Structure Interaction, LNCSE, Vol. 53, pp. 146-170, 2006.

[26] D. Cerroni, S. Manservisi and F. Menghini, *An improved monolithic multigrid Fluid-Structure Interaction solver with a new moving mesh technique*, International Journal of Mathematical Models and Methods in Applied Sciences, Vol. 9, pp. 227-234, 2015.

[27] J.H. Bramble, *Multigrid methods*, Pitman Research Notes in Math, 294, Longman, London, 1993.